THE JOURNAL OF BIOLOGICAL CHEMISTRY VOL. 280, NO. 50, pp. 41675–41682, December 16, 2005

Structure and Substrate Specificity of the Pim-1 Kinase*

Received for publication, September 30, 2005, and in revised form, October 12, 2005 Published, JBC Papers in Press, October 13, 2005, DOI 10.1074/jbc.M510711200

Alex N. Bullock[‡], Judit Debreczeni[‡], Ann L. Amos[‡], Stefan Knapp[‡], and Benjamin E. Turk[§1]

From the [‡]Oxford University, Centre for Structural Genomics, Botnar Research Centre, Oxford OX3 7LD, United Kingdom and the [§]Department of Pharmacology, Yale University School of Medicine, New Haven, Connecticut 06520

The Pim kinases are a family of three vertebrate protein serine/threonine kinases (Pim-1, -2, and -3) belonging to the CAMK (calmodulin-dependent protein kinase-related) group. Pim kinases are emerging as important mediators of cytokine signaling pathways in hematopoietic cells, and they contribute to the progression of certain leukemias and solid tumors. A number of cytoplasmic and nuclear proteins are phosphorylated by Pim kinases and may act as their effectors in normal physiology and in disease. Recent crystallographic studies of Pim-1 have identified unique structural features but have not provided insight into how the kinase recognizes its target substrates. Here, we have conducted peptide library screens to exhaustively determine the sequence specificity of active site-mediated phosphorylation by Pim-1 and Pim-3. We have identified the major site of Pim-1 autophosphorylation and find surprisingly that it maps to a novel site that diverges from its consensus phosphorylation motif. We have solved the crystal structure of Pim-1 bound to a high affinity peptide substrate in complexes with either the ATP analog AMP-PNP or the bisindolylmaleimide kinase inhibitor 2-[1-(3-dimethylaminopropyl)-1H-indol-3-yl]-3-(1H-indol-3-yl)maleimide HCl. These structures reveal an unanticipated mode of recognition for basic residues upstream of the phosphorylation site, distinct from that of other kinases with similar substrate specificity. The structures provide a rationale for the unusually high affinity of Pim kinases for peptide substrates and suggest a general mode for substrate binding to members of the CAMK group.

Pim-1 was first described with c-*myc* as a frequent proviral insertion site in Moloney murine leukemia virus-induced T-cell lymphomas (1, 2). Activation of the two oncogenes is strongly cooperative, such that double-transgenic Eμ-*myc* Eμ-*pim1* mice exhibit pre-B-cell leukemia *in utero* (3). Likewise, activating proviral insertion in the *pim2* and *pim3* genes can also contribute to leukemia in the mouse (4, 5). Pim-1 overexpression is observed in a range of human lymphomas and acute leukemias (6), whereas Pim-2 overexpression is associated with chronic lymphocytic leukemia and non-Hodgkin lymphoma (7). Pim-1 is also a prognostic marker in prostate cancer (8, 9), and Pim-3 shows aberrant expression in hepatocellular carcinoma (10). Additionally, *pim1* somatic hypermutations (11) and chromosomal translocations have been identified in non-Hodgkin lymphoma (12). In light of their oncogenic potential, the Pim kinase family is emerging as an important new target for drug discovery efforts (13–15).

Physiologically, Pim kinases appear to contribute to the proliferation and survival of leukocytes. Pim-1 and Pim-2 are expressed at low levels in many tissues but are strongly induced in leukocytes by the JAK/STAT[2] pathway in response to cytokines, including interleukins 2, 3, and 7, granulocyte-macrophage colony-stimulating factor, α- and γ-interferon, and erythropoietin (16–18). Pim kinase regulation appears to be largely at the level of transcription; kinase activity correlates with protein levels, and there is no evidence for regulation by post-translational modification (19, 20). Mice harboring targeted knockouts of all three *pim* genes develop normally but display reduced body size owing to decreased cell number in virtually all tissues (21), suggesting a direct role in controlling cell proliferation in cells outside the hematopoietic system as well.

Pim kinases contribute to both cell proliferation and survival and thus provide a selective advantage in tumorigenesis. A number of proteins have been identified that are phosphorylated by Pim kinases *in vitro*, including transcriptional repressors (HP1), activators (NFATc1 and c-Myb), and co-activators (p100), as well as regulators of the cell cycle ($p21^{WAF1/CIP1}$, Cdc25A phosphatase, and the kinase C-TAK1/MARK3/Par1A) (22–28). The status of any of these proteins, however, as *bona fide* effectors of Pim kinases *in vivo* has not been established. Pim kinases appear to phosphorylate the pro-apoptotic protein BAD both *in vitro* and *in vivo* on Ser-112, a gatekeeper residue for its inactivation, and induce apoptotic resistance under conditions of growth factor withdrawal (20, 29, 30). Finally, Pim-1 is reported to modulate a cytokine negative feedback mechanism by preventing the proteasomal degradation of SOCS-1, which may be mediated by direct phosphorylation (31).

The substrate specificity of Pim-1 and Pim-2 is characterized by strong preferences for basic residues at positions −5 and −3 and a small side chain at +1 (32–34). Interestingly, selectivity for arginine at the −5 and −3 positions within substrates is also a feature of Akt/PKB, a downstream mediator of cell survival in phosphoinositide 3-kinase signaling (35, 36). Akt/PKB and Pim kinases appear to play redundant roles in mediating hematopoietic cell growth and survival, possibly due to overlapping substrates, including BAD, $p21^{WAF1/CIP1}$, and Cot/Tpl-2 (28, 37, 38). Comprehensive peptide library screening with Pim-2 has indicated secondary selectivity for particular residues at other positions, which has allowed the generation of peptide substrates selective for Pim kinases over Akt/PKB (34).

Several groups have recently reported the x-ray crystal structure of Pim-1 in complex with nucleotide analogs and a number of small molecule ATP-competitive inhibitors (14, 39, 40). Their studies revealed a constitutively active kinase conformation in the absence of phosphoryl-

* The Structural Genomics Consortium is a registered charity (number 1097737) funded by the Wellcome Trust, GlaxoSmithKline, Genome Canada, the Canadian Institutes of Health Research, the Ontario Innovation Trust, the Ontario Research and Development Challenge Fund, and the Canadian Foundation for Innovation. The costs of publication of this article were defrayed in part by the payment of page charges. This article must therefore be hereby marked "*advertisement*" in accordance with 18 U.S.C. Section 1734 solely to indicate this fact.

The atomic coordinates and structure factors (codes 2BIL, 2BZK, and 1XWS) have been deposited in the Protein Data Bank, Research Collaboratory for Structural Bioinformatics, Rutgers University, New Brunswick, NJ (http://www.rcsb.org/).

[1] A Leukemia and Lymphoma Society Special Fellow. To whom correspondence should be addressed: Dept. of Pharmacology, Yale University School of Medicine, P. O. Box 208066, 333 Cedar St., New Haven, CT 06520. Tel.: 203-737-2494; Fax: 203-785-7670; E-mail: ben.turk@yale.edu.

[2] The abbreviations used are: JAK/STAT, Janus kinase/signal transducers and activators of transcription; PKB, protein kinase B; CAMK, calmodulin-dependent protein kinase; ESI-MS, electrospray ionization mass spectrometry; DTT, dithiothreitol; BIM1, 2-[1-(3-dimethylaminopropyl)-1H-indol-3-yl]-3-(1H-indol-3-yl)maleimide HCl; ITC, isothermal titration calorimetry; AMP-PNP, adenosine 5′-(β,γ-imino)triphosphate.

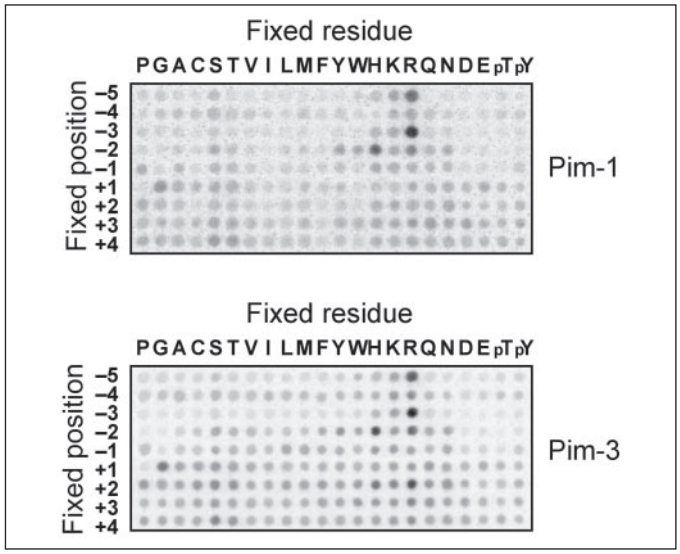

FIGURE 1. **Phosphorylation motifs for Pim-1 and Pim-3.** Biotinylated peptides bearing the indicated residue at the indicated position relative to a central Ser/Thr phosphoacceptor site were subjected to phosphorylation by the kinase using radiolabeled ATP. Aliquots of each reaction were subsequently spotted onto a streptavidin membrane, which was washed, dried, and exposed to a phosphor screen.

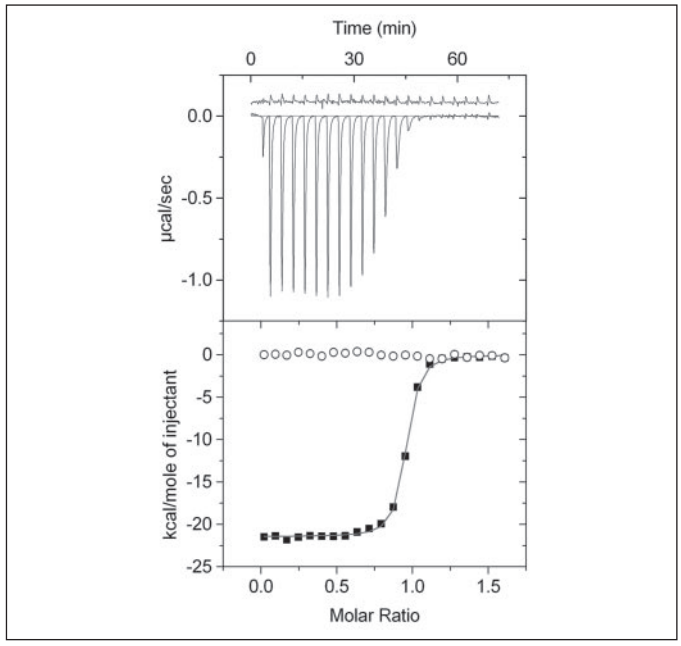

FIGURE 2. **Determination of Pim kinase affinities for peptide substrates by ITC.** Raw data of a titration experiment (*top trace*) and a blank titration (*bottom trace*) for Pim-1 with Pimtide are shown in the *upper panel*, and normalized data after baseline subtraction are shown in the *lower panel*. Non-linear least squares fit analysis provided the thermodynamic data and binding constants as shown in TABLE ONE.

ated residues in the activation loop. In addition, the Pim-1 structures revealed a unique hinge region lacking a hydrogen bond donor, suggesting potential for the development of specific Pim kinase inhibitors that target the ATP binding site. We have extended these structural studies to provide insight into the molecular basis for substrate recognition by Pim-1. Comparison of the previously determined Pim-2 phosphorylation motif with new peptide library screens performed on Pim-1 and Pim-3 indicates that the three Pim kinases share a common consensus sequence. Accordingly, we have found that the optimized peptide previously described for Pim-2 is also a high affinity substrate for Pim-1, enabling crystallographic studies of Pim-1·peptide complexes. Comparison with the previously determined crystal structure of an Akt/PKB·AMP-PNP·peptide complex (41), as well as those of three other solved serine/threonine kinase·substrate complexes (42–44) reveals a previously undescribed mode of substrate recognition for Pim-1 that may share features with other members of the calmodulin-dependent protein kinase (CAMK) family.

EXPERIMENTAL PROCEDURES

Protein Expression and Purification—Full-length human Pim-1 (36-kDa isoform, gi 33304198) was subcloned by ligation-independent cloning into a pET-derived expression vector, pLIC, and expression performed in BL21(DE3) with 1 mM isopropyl 1-thio-β-D-galactopyranoside induction for 4 h at 18 °C. Cells were lysed using a high pressure homogenizer and cleared by centrifugation, and the lysate was purified by nickel-nitrilotriacetic acid chromatography. The eluted Pim-1 protein was treated with λ-phosphatase together with tobacco etch virus (TEV) protease overnight to remove phosphorylation and the hexahistidine tag, respectively. The protein was further purified on a Mono Q column and resolved into two species, shown by ESI-MS to be homogeneous non-phosphorylated and singly phosphorylated Pim-1. Protein was stored at 4 °C in elution buffer (50 mM HEPES, pH 7.5, 250 mM NaCl, 5% glycerol, and 10 mM DTT) or frozen in liquid nitrogen and stored at −80 °C.

Determination of Peptide Phosphorylation Specificity—Phosphorylation motifs for Pim kinases were determined using a positional scanning peptide library approach essentially as described previously (34). Reactions were carried out in multiwell plates in 20 mM HEPES, pH 7.4, 10 mM $MgCl_2$, 1 mM DTT, 0.1% Tween 20, 50 μM ATP (including 0.3 μCi/μl [γ-^{33}P]ATP), 50 μM peptide substrate, and 300 nM Pim kinase for 2–4 h at 30 °C. Peptide substrates had the general sequence YA*XXXXX*(S/T)*XXXX*AGKK(biotin), where S/T represents an even mixture of serine and threonine, K(biotin) is ε-(biotinamidocaproyl)-lysine, and is a roughly equimolar mixture of the 17 amino acids, excluding cysteine, serine, and threonine. Each well contained a distinct peptide in which one of the X positions was fixed as one of 22 residues (one of the unmodified proteogenic amino acids, phosphothreonine, or phosphotyrosine). At the end of the incubation time, aliquots of each reaction were spotted onto streptavidin membrane, which was processed as described (34). Phosphorylation of Pimtide by Pim-1 was assayed by P81 phosphocellulose filter binding as described using 9 pM Pim-1 for 5–10 min at 30 °C. Initial rates were measured at peptide substrate concentrations of 12.5, 25, 50, 100, 200, 400, and 800 nM and an ATP concentration of 25 μM to determine the K_m value. Reaction progress was linear over time.

Autophosphorylation—Reactions were initiated at room temperature by the addition of 5 μM (final concentration) non-phosphorylated Pim-1 to a 200-μl solution containing 50 mM HEPES, pH 7.5, 100 mM NaCl, 5 mM DTT, 1 mM ATP, 5 mM $MgCl_2$, and 0.5 mM $MnCl_2$. At each time point a 5-μl aliquot was removed and added to a stop buffer containing 20 mM EDTA and 0.1% formic acid. Protein masses were determined by liquid chromatography-MS, using an Agilent LC/MSD TOF system with reversed-phase high-performance liquid chromatography coupled to electrospray ionization and an orthogonal time-of-flight mass analyzer. Proteins were desalted prior to mass spectrometry by rapid elution off a C3 column with a gradient of 5–95% acetonitrile in water with 0.1% formic acid. Spectra were analyzed and exported using Analyst QS (Agilent) and transformed using MagTran.

Isothermal Titration Calorimetry—Calorimetric measurements were carried out using a VP-ITC titration calorimeter (MicroCal, Inc.). Peptides (100–500 μM) were titrated into Pim-1 protein (10 μM) buff-

TABLE ONE

ITC data for Pim-1 binding to peptide substrates at 10 °C

Complex	K_D	$K_a \times 10^4$	ΔH^{obs}	$T\Delta S$	ΔG	N[a]
	μM	M^{-1}	kcal/mol			
Pim-1 + Pimtide[b]	0.058	2100 ± 1400	−16.5 ± 0.2	−7.1	−9.3	1.0
Pim-2 + Pimtide[c]	0.64	160 ± 20	−13.4 ± 0.4	−5.4	−8.0	1.3
Pim-3 + Pimtide	0.039	2580 ± 214	−13.7 ± 0.06	−4.08	−9.62	1.2
Pim-1 + p21tide	28	3.61 ± 0.92	−7.77 ± 5.71	−1.86	−5.91	0.91
Pim-1 + PAP-1tide	37	2.67 ± 1.34	−3.42 ± 4.39	2.33	−5.75	2.30

[a] Stoichiometry was determined from a single binding site model.
[b] Average from two separate determinations.
[c] Average from three separate determinations.

ered in 50 mM HEPES, pH 7.5, 150 mM NaCl, and 1 mM DTT. Heats of dilution were measured in blank titrations and were subtracted from the binding heats. Data were analyzed using a single binding site model implemented in the Origin software package provided with the instrument. Peptides were synthesized by Thermo Electron GmbH and purified by reversed-phase high-performance liquid chromatography (Pimtide: ARKRRRHPSGPPTA-amide; p21tide: RKRRQTSMTD; PAP-1tide: KKRKHKASKSS).

Crystallization—Non-phosphorylated Pim-1 (buffered in 50 mM HEPES, pH 7.5, 250 mM NaCl, 5% glycerol, and 10 mM DTT) was concentrated to 5–8 mg/ml in the presence of bound ligands (theoretical final concentrations: 0.6 mM Pimtide, and either 0.6 mM BIM1 or 1 mM AMP-PNP-$MgCl_2$. BIM1 (2-[1-(3-dimethylaminopropyl)-1H-indol-3-yl]-3-(1H-indol-3-yl)maleimide HCl) was purchased from Calbiochem and added from a 50 mM Me_2SO stock solution. Co-crystals were grown at 4 °C in 150-nl sitting drops mixing 100 nl of Pim-1 ligand complex with a 50-nl precipitant. The Pim-1·BIM1·Pimtide co-crystal grew from a precipitant solution containing 0.1 M SPG (pH 6.0, mix ratio 2:7:7 succinate/sodium phosphate/glycine), 30% polyethylene glycol 1000, 0.5% Me_2SO. The Pim-1·AMP-PNP·Pimtide co-crystal grew from a precipitant solution containing 0.2 M NH_4Cl pH 6.3, 20% polyethylene glycol 3350.

Structure Determination—Pim-1 diffraction data were collected on a frozen crystal (100 K) using a Rigaku FRE x-ray generator equipped with multilayer mirrors and an R-AXIS HTC detector. Images were indexed and integrated using MOSFLM (45), and scaled using SCALA (46) implemented in the CCP4 (47) suite of programs. The structures were solved using molecular replacement and the program Phaser (48) with coordinates of Pim-1 in complex with BIM1 (Protein Data Bank (PDB) code 1XWS). Both structures were refined with REFMAC5 (49) using iterative rounds of rigid-body refinement and restrained refinement with TLS, against maximum likelihood targets, interspersed with manual rebuilding of the model using Xfit/XtalView (50).

Coordinates—Coordinates for Pim-1 in complex with the bisindolylmaleimide inhibitor BIM1 and Pim-1 consensus peptide as well as AMP-PNP and Pim-1 consensus peptide have been deposited in the Protein Data Bank (PDB codes 2BIL and 2BZK, respectively).

RESULTS

The Three Pim Kinases Share a Common Phosphorylation Consensus Sequence—Based on analysis of individual peptide substrates, Pim-1 has been described as having selectivity for basic residues at the −5 through −2 positions relative to the phosphorylation site and for smaller residues at the +1 position (32, 33). Recently we used a peptide library approach to systematically evaluate the contribution of all amino acid residues at each of nine positions surrounding a fixed phosphoacceptor site to phosphorylation by Pim-2 (34). Although most closely related to

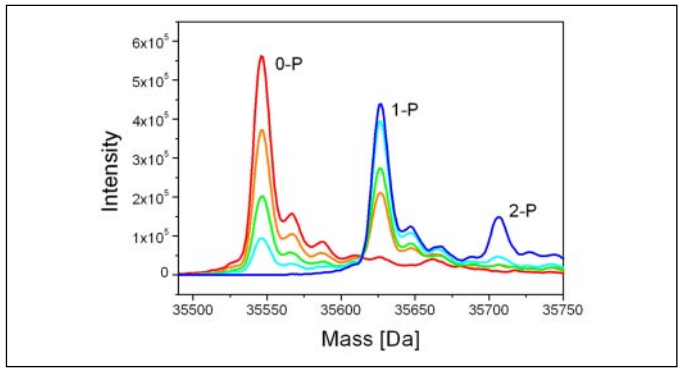

FIGURE 3. **Kinetics of autophosphorylation monitored by ESI-MS.** Shown are ESI-MS spectra recorded during different time points of the autophosphorylation experiment and colored as follows: 0 min (*red*), 5 min (*orange*), 10 min (*green*), 20 min (*cyan*), and 300 min (*blue*). Peaks corresponding to the mass sizes of non-phosphorylated, singly phosphorylated, and doubly phosphorylated Pim-1 are indicated by the labels *0-P*, *1-P*, and *2-P*, respectively.

the other Pim kinases, human Pim-2 is only 61 and 66% identical within its catalytic domain to Pim-1 and Pim-3, respectively, suggesting that there may be differences in substrate specificity among members of the family. To determine if this were the case, we repeated the peptide library screens using bacterially expressed Pim-1 and Pim-3 (Fig. 1). The phosphorylation profile of both Pim-1 and Pim-3 is overall very similar to that of Pim-2, including both major and secondary selections. In addition to a strong preference for basic residues, particularly arginine, at the −5 and −3 positions, the common Pim kinase motif is characterized by selectivity at a number of other sites, including histidine at the −2, proline at the −1, and glycine at the +1 positions.

A consensus peptide substrate, Pimtide (ARKRRRHPSGPPTA), was previously generated based on the peptide library results and shown to be efficiently phosphorylated by Pim-2 (34). As a prelude to structural studies, we determined the binding affinity of this peptide to the various Pim kinases by ITC (Fig. 2). Both Pim-1 and Pim-3 bind to Pimtide with strikingly high affinity, having K_D values in the range of 40–60 nM (TABLE ONE). Binding is driven strongly by enthalpy as expected by the large number of polar interactions in the peptide protein interface. Limitations in the sensitivity of standard radiolabel kinase assays made it difficult to accurately measure the atypically low K_m value for Pimtide phosphorylation by Pim-1. We were able to determine this value to be below 100 nM and on the same order as the binding constant ($K_m = 34 \pm 6$ nM, $n = 3$). By comparison, the affinity of Pimtide for Pim-2 is somewhat weaker (0.64 μM), consistent with its higher reported K_m value (1.2 μM) as a Pim-2 substrate (34). Compared with Pimtide, the binding affinities for Pim-1 of phosphorylation site peptides derived from two Pim-1 substrates, $p21^{WAF1/CIP1}$ and PAP-1, are approximately three orders of magnitude weaker. Likewise, ribosomal protein S6-derived

TABLE TWO

Crystallographic data and refinement statistics

Data collection	BIM1/Pimtide	AMP-PNP/Pimtide
Space group	$P6_5$	$P6_5$
Cell dimensions (Å)	a, b = 98.1, c = 80.04	a, b = 97.89, c = 80.49
Resolution (Å)	2.55	2.45
Total observation (unique, redundancy)	97,016 (14,259, 6.7)	119,106 (16,216, 7.3)
Completeness (outer shell)	98.9 (96.7)	100 (99.5)
R_{merge} (outer shell) (%)	7.2 (36)	7.1 (55)
I/σ (outer shell)	9.7 (2.2)	9.4 (3.2)
Refinement		
R_{work} (R_{free})[a] (%)	19.2 (24.8)	19.2 (22.5)
Hetero groups	BIM-1	AMP-PNP
r.m.s.d. bond length (Å)	0.017	0.013
r.m.s.d. bond angle (°)	1.979	1.45
Number of atoms		
Protein (residues)[b]	2,264 (275)	2,235 (281)
Heterogroups (atoms)	30	31
Water molecules	48	23
Ramachandran		
Allowed/generally allowed/disallowed	92.4%/7.6%/0%	94%/6.0%/0%

[a] R_{free} was calculated using 5% of the data assigned randomly.
[b] Residues 46–50 were not defined in the electron density.

peptides of similar length often used to assay Pim-1 activity have reported K_m values ranging from 6–13 μM (33). By comparison, other kinases in the CAMK group have K_m values for optimized peptide substrates that are typically in the 5–10 μM range (51).

Pim-1 Autophosphorylates at a Non-consensus Site in Vitro—Human Pim-1 is multiply phosphorylated upon expression in *Escherichia coli*. The major autophosphorylation site has been mapped to Ser-261(*) within the sequence RQRVSS*ECQHL, which conforms well to the Pim-1 consensus, containing arginine at both −5 and −3 (39). Following limited dephosphorylation with λ-phosphatase, this singly phosphorylated species can be resolved from fully dephosphorylated Pim-1 by Mono Q ion exchange chromatography. Autophosphorylation was followed *in vitro* using non-phosphorylated Pim-1 protein by electrospray ionization mass spectrometry (ESI-MS, Fig. 3). A single autophosphorylation event was rapidly detected with a half-time of 5–10 min, and a second phosphorylation did not accumulate to more than ~20% after 5-h incubation. Surprisingly, the major *in vitro* autophosphorylation site was not detected at Ser-261 but was mapped to Ser-8(*) in the unstructured protein N terminus within the sequence LSKINS*LAHLR by mass spectrometry (data not shown). To confirm this result the *in vitro* autophosphorylation was repeated using the singly Ser-261-phosphorylated Pim-1 protein. Identical phosphorylation kinetics were observed, indicating that Ser-261 phosphorylation may be an artifact of bacterial expression and that the Pim-1 N terminus may be a more likely authentic autophosphorylation site *in vivo*. Autophosphorylation during expression in bacteria is likely to occur in trans either co-translationally or immediately post-translationally, while the protein is incompletely folded. In the folded protein, Ser-261 is the first residue of helix αH in the C-terminal lobe, where its helical conformation presumably renders it inaccessible to subsequent phosphorylation. Phosphorylation at Ser-261 appears to have no effect on conformation or activity (15, 39). Whether phosphorylation at Ser-8 impacts inherent kinase activity is not clear, but it could mediate interactions with other proteins or affect Pim-1 stability and/or localization within cells. These results with human Pim-1 are in contrast to previous reports with the *Xenopus* ortholog, in which the major autophosphorylation site was identified as Ser-189 and are likely to reflect differences between the mammalian and reptilian proteins (52).

Structures of Pim-1 in Complex with a Consensus Peptide and ATP Site Inhibitors Reveal a Unique Mode of Substrate Recognition for a Basophilic Kinase—To understand the structural basis for substrate selectivity by Pim kinases, we solved the x-ray crystal structure of Pim-1 in complex with the Pimtide substrate. Pim-1 was co-crystallized with peptide along with either the bisindolylmaleimide inhibitor BIM1 or the ATP analog AMP-PNP (TABLE TWO). As reported previously (14, 39, 40), Pim-1 adopts a typical bi-lobed kinase fold, with several unique features (Fig. 4). Most notably, the hinge region (residues 121–126) has an unusual conformation owing to a 1–2 residue insertion and the presence of two proline residues that serve to widen the ATP-binding pocket. As anticipated based on assay of kinase activity, unphosphorylated Pim-1 appears to be in an active conformation, with residues at the active site positioned appropriately to catalyze phosphate transfer. This constitutively active conformation is probably stabilized by polar interactions between Asp-200 in the activation loop and Arg-166 (the residue that precedes the catalytic aspartate), as well as multiple hydrophobic interactions involving residues within the activation loop and the C-terminal lobe of the kinase.

In both structures, the main chain of residue 3 plus the entirety of residues 4–9 in the peptide (corresponding to the −6 position through the serine at position 0) were well ordered in the crystal structure, whereas the remainder of the peptide was disordered (Fig. 4). As for other serine-threonine kinases whose structures have been determined in complex with peptide substrates, the substrate binds in a largely extended conformation within a cleft in the C-terminal lobe of the kinase, with the peptide backbone making a turn at the −3 residue (Fig. 5). The hydroxyl group of the serine phosphoacceptor makes a hydrogen bond to Asp-167, the residue that acts as a proton acceptor during phosphate transfer, suggesting that the peptide is bound in a mode that would be productive for catalysis. Comparison of the ternary Pim-1·BIM1·Pimtide complex with Pim-1 bound to BIM1 alone (15) (PDB code 1XWS) indicates that the backbone conformation of Pim-1

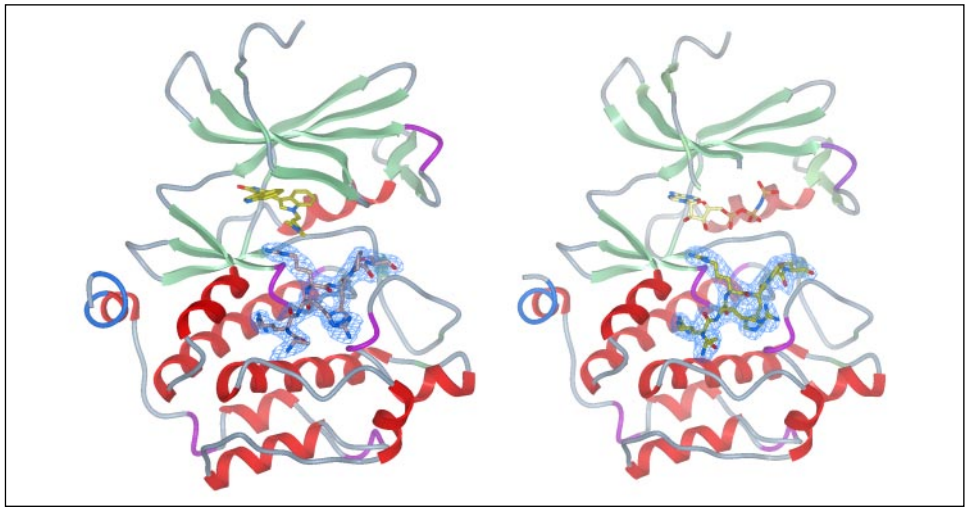

FIGURE 4. **Structural overview of the Pim-1·BIM1·peptide complex (*left*) and the Pim-1·AMP-PNP·peptide complex (*right*).** BIM1 and AMP-PNP are shown in *stick representation* with *yellow* carbon atoms. The electron density (1σ) around the peptide is shown in *blue*. Residues 46–50 were not defined in the electron density of the AMP-PNP complex. The figure was generated using ICM (65).

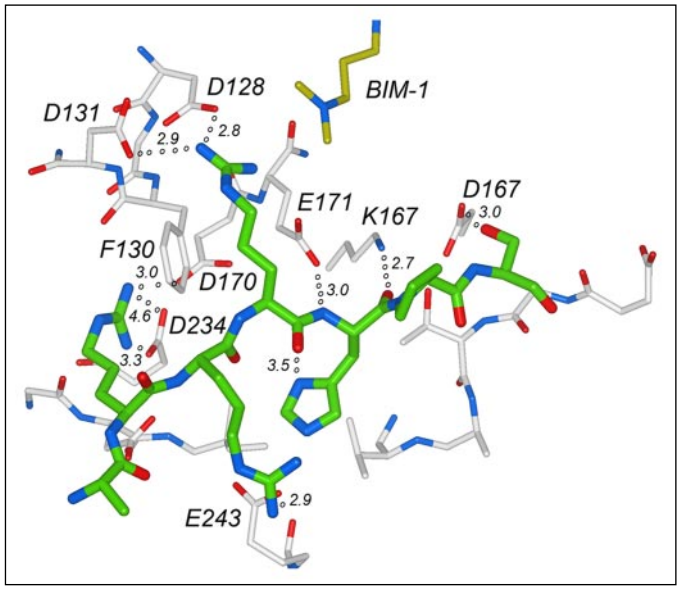

FIGURE 5. **Peptide binding site with interacting residues for the Pim-1·BIM1 complex.** Distances are shown in angstroms. BIM1 is highlighted using *yellow* carbon atoms.

changes very little upon peptide binding (root mean square deviation 0.3 Å).

In the two previously reported structures of Pim-1 in complex with AMP-PNP, the glycine-rich loop of the ATP binding site adopted distinct conformations (14, 40). Qian *et al.* reported that this loop undergoes a significant conformational change upon nucleotide binding and is in a relatively open conformation. In the structure by Kumar *et al.*, the loop more closely resembles the structure of the apoenzyme, with the γ-phosphate of AMP-PNP participating in a network of polar contacts, suggestive of a pre-catalytic complex. In the ternary complex with AMP-PNP and peptide, we find that the G-loop is completely disordered, consistent with flexibility of this region of the kinase. The nucleotide analog adopts a non-catalytic conformation, with the γ-phosphate group pointed away from the active site (Fig. 4).

The basis for Pim-1 selection of basic residues at the −3 and −5 positions in its substrates is apparent from inspection of the structures (Fig. 5). The side chain of the −3 arginine residue extends into the cleft between the N- and C-terminal lobes of the kinase, where its guanidinium head group makes polar contacts with multiple acidic residues, and its aliphatic stalk packs against Phe-130 from the αD helix. The shallow pocket formed by these residues is a conserved feature of so-called basophilic kinases within the AGC and CAMK groups that select substrates with arginine residues at the −3 position (41, 43, 44). In particular, all such kinases have a hydrophobic residue (typically Phe, Leu, or Met) at the position analogous to Phe-130, and all have an acidic residue at the position analogous to Asp-128 (TABLE THREE). The head group of the −3 arginine residue of Pimtide, however, makes polar contacts with two additional acidic residues (Asp-131 and Glu-171) found within the pocket of Pim-1 that are not as widely conserved.

The −5 arginine residue interacts with a number of residues in a distinct pocket separated from the −3 binding site by Phe-130. These include the hydroxyl group of Thr-134, the backbone carbonyl group of Gly-238, and the carboxyl groups of three acidic residues (Asp-170, Asp-234, and Asp-239). Pim kinases share their preference for arginine at the −5 position in substrates with several members of the AGC kinase group, notably Akt/PKB (35). Comparison of our Pim-1·peptide structures with the reported crystal structure of an Akt2·AMP-PNP·peptide complex (41), however, reveals significant differences in the manner in which these two kinases interact with their substrates (Fig. 6). Although the backbone conformation of the bound peptide is similar in the two structures, the side chain of the −5 arginine residue occupies distinct sites that have only one residue in common (Asp-234 in Pim-1, corresponding to Glu-342 in Akt2). In Akt2, the guanidinium headgroup makes an additional bidentate salt bridge with Glu-279. The analogous residue in protein kinase A makes a similar ion pair with the arginine residue found at the −2 position in its substrates (44, 53). Although this glutamate residue is conserved in Pim-1 (Glu-171), as noted above it participates instead in interactions with the −3 substrate residue.

Interactions between other residues in the peptide and the enzyme are less extensive, consistent with less stringent selectivity for Pim kinases outside of the −5 and −3 positions. Glu-243 becomes positioned to make polar contacts with the headgroups of both the −2 His and −4 Arg residues in the bound peptide. The conformation of the −4 Arg side chain differs slightly between the BIM1 and ANP-PNP complexes, with Glu-243 interacting with the guanidinium group at different points. Notably, Glu-243 is the only residue in Pim-1 that changes conformation upon substrate binding to interact with the peptide. The −1 Pro side chain does not appear to contact the enzyme directly.

No density is visible in either structure for Pimtide residues downstream of the phosphorylation site, suggesting that they do not make extensive contact with the kinase. This is consistent with the general

TABLE THREE

Specificity determining residues for Pim-1 and related kinases

	−5 Specificity	Interacting residues (Pim-1 numbering)								
		−5 Interacting				−3 Interacting				−2/−4
		134	170	234	239	128	130	131	171	243
Pim-1	Arg/Lys	Thr	Asp	Asp	Asp	Asp	Phe	Asp	Glu	Glu
Pim-2	Arg/Lys	Thr	Asp	Asp	Asp	Asp	Phe	Asp	Glu	Glu
Pim-3	Arg/Lys	Thr	Asp	Asp	Asp	Asp	Phe	Asp	Glu	Glu
PASK	?	Asp	Asp	Thr	Glu	Asp	Phe	Ala	Glu	Cys
PKD1	Leu/Val/Ile	Leu	Pro	Val	Thr	Asp	Leu	Glu	Glu	Asn
MK2	Leu/Phe/Ile	Gln	Pro	Ile	Tyr	Glu	Phe	Ser	Glu	Tyr
CAMK1	Leu/Ile/Phe	Val	Pro	Ile	Tyr	Glu	Phe	Asp	Glu	Tyr
PhK1	*X*	Thr	Pro	Thr	Ser	Glu	Phe	Asp	Glu	Trp
Akt2	Arg	Ser	Leu	Glu	Arg	Glu	Phe	Phe	Glu	Tyr

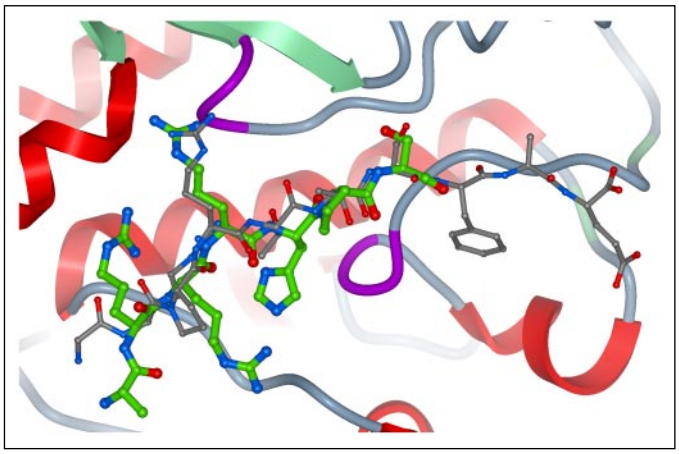

FIGURE 6. **Comparison of peptide substrates bound to Pim-1 and Akt/PKB.** The figure shows an overlay of the glycogen synthase kinase-derived substrate peptide (*gray*, sequence GRPRTTSFAE) from the complex with Akt/PKB (PDB code 1O6L) and Pimtide (*green*) on a *ribbon diagram* of Pim-1 kinase. The lower lobes of the two kinases have been superimposed. The arginine residues at the −3 position occupy analogous binding sites, but the residues at −5 do not.

lack of selectivity at the downstream positions and with previous observations that deletion of these residues in peptide substrates does not affect Pim-1 catalytic efficiency (33). The Pim-1 structure provides a potential rationale for these observations. In complexes between peptide substrates and other basophilic kinases (protein kinase A, Akt, and phosphorylase kinase), the residue in the +1 position of the substrate makes antiparallel β-sheet-like hydrogen bonds to the main chain of an activation loop glycine residue corresponding to Gly-203 in Pim-1. Interestingly, in Pim-1, this residue is rotated ~180° about its C^{α}–N bond, rendering the amide inaccessible as a hydrogen bond donor to the substrate (Fig. 7). This conformation appears to be stabilized in part by an interaction between the backbone carbonyl of the residue immediately upstream (Asp-202) and the side chain of Ser-189 at the start of the activation loop. As noted by Shaw and co-workers (54, 55) for other kinases belonging to the AGC and CAMK groups, Pim kinases appear to strongly deselect Pro in the +1 position in substrates. This "proline disfavor" phenomenon is generally attributable to the inability of Pro to hydrogen bond to the carbonyl group of the residue equivalent to Gly-203 in the kinase. In the case of Pim-1 this rationale seems unlikely, because the +1 residue in Pimtide does not appear to contact Gly-203. Proline deselection by Pim kinases may be instead due to steric clashes that would preclude the serine phosphoacceptor from assuming a conformation competent for phosphate transfer.

DISCUSSION

Although they belong to a different kinase group (CAMK), the Pim kinases have overlapping substrate specificity with Akt/PKB and other AGC kinases, in particular for arginine residues at the −5 position. We have found, however that this residue binds to a pocket in Pim-1 distinct from its binding site in Akt/PKB. The alternate binding mode for basic residues used by Pim-1 is surprising in light of the fact that all of the residues in Akt that interact with the two arginine residues are conserved among Pim kinases (TABLE THREE). The extensive network of ionic and polar contacts made between Pim-1 and its peptide substrate provides a rationale for why the observed mode of interaction is preferred to the "Akt" binding mode and for the extraordinarily high affinity of Pim-1 for the Pimtide substrate.

Interestingly, among all human protein kinases, only the Pim kinases have acidic residues at all three positions that interact with the −5 arginine residue in Pim-1 (56). Only two other kinases (Per-Arnt-Sim (PAS) kinase, the closest relative to the Pim kinases, and STK33) have acidic residues at two of the three positions. Other CAMKs that have been characterized thus far are either relatively nonselective or prefer non-polar residues at the −5 position (57–61). The identity of the residue analogous to position 234 in Pim-1 in particular seems to correlate with selectivity. Kinases that prefer hydrophobic residues at −5, such as protein kinase D, MAP kinase-activated protein kinase 2, and CAMK1, have aliphatic residues at this position, whereas phosphorylase kinase, which is less selective, has a polar threonine residue (TABLE THREE). These correlations point to the likelihood of a common binding site among CAMKs for the −5 residue in substrates. Based on the absence of acidic residues at these positions among other CAMKs, it is probable that within this group only the Pim kinases are highly selective for arginine at the −5 position.

Implications for Pim Kinase Substrate and Inhibitor Selectivity—Each of the residues in Pim-1 that make contact with the bound peptide is identical in Pim-2 and Pim-3 (TABLE THREE), explaining the similarity between the phosphorylation motifs of these three kinases. Although most Pim kinase protein substrates have not been tested for their ability to be phosphorylated by multiple members of the family, those that have (BAD and Socs-1) appear to be efficient substrates for each kinase. Studies with mice deficient in multiple Pim kinases indicate some redundancy between the different family members. However, it is clear that loss of particular Pim kinases in some contexts is not compensated by the presence of others (21). For example, interleukin-3-dependent growth of bone marrow-derived mast cells is specifically reduced with Pim-1 deficiency, despite substantial Pim-2 induction by interleukin-3 (62). Likewise, loss of Pim-2 specifically impairs the growth and survival

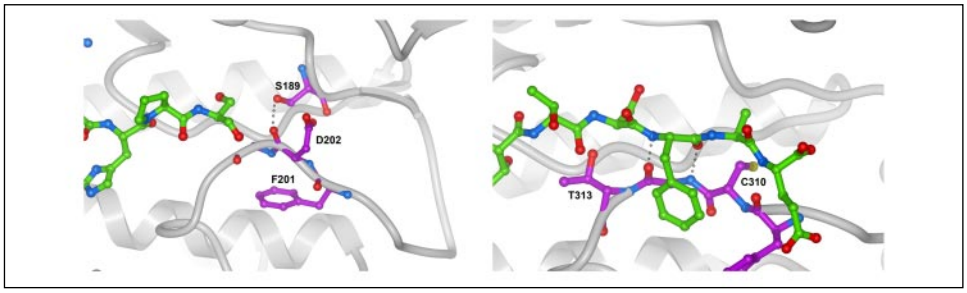

FIGURE 7. **Unusual activation loop conformation for Pim-1.** The region of the activation loop near the binding site for +1 residues is shown in stick representation for Pim-1 (*left*) and Akt/PKB (*right*). Bound peptide substrates are shown in *green*. Pim-1 residues are shown in *magenta*. The interaction between the Ser-189 hydroxyl and the Asp-202 backbone carbonyl groups in Pim-1 is indicated. The sheet-like interactions between the +1 Phe in the substrate and the Gly-203 equivalent in Akt are shown on the *right*; in Pim-1 the Gly-203 amide NH is pointed in the opposite direction and cannot accept a hydrogen bond from the substrate. The figure was generated using ICM (65).

of T lymphocytes (21, 37, 63). These observations suggest that specific substrates exist for each of the Pim kinases. Phosphorylation of specific substrates could be mediated by interactions outside of the active site either directly with the kinase or through intermediary scaffolding proteins, possibly involving recruitment to distinct subcellular locales.

The unusual primary structure and conformation of the Pim-1 hinge region gives rise to a wider ATP binding pocket lacking a conserved hydrogen bond donor that can participate in inhibitor binding. Despite this, a recent screen of a directed small molecule library identified potent Pim-1 inhibitors among compounds with common kinase inhibitor scaffolds, including bisindolylmaleimides and flavonoids (15). Other potential avenues for the generation of high affinity Pim kinase inhibitors are suggested by the work presented here. The unusually low dissociation constant for the Pimtide substrate suggests the possibility of discovering potent inhibitors that target the peptide binding site. Tethered bivalent inhibitors that link an ATP-competitive inhibitor to a peptide substrate analog would be anticipated to have both increased specificity and potency over standard inhibitors. Such molecules are typically prepared by tethering an ATP analog to the peptide by way of the phosphoacceptor site (64). In the structure of the complex with peptide and BIM1, it is notable, however, that the guanidinium group of the −3 arginine residue comes in close proximity to the dimethylamino group of the bound inhibitor (3.4 Å). This proximity suggests a potential alternative linkage strategy for the construction of a bivalent inhibitor that may increase specificity for Pim-1 over other kinases. The development of specific inhibitors will be a valuable tool for dissecting the biological roles of Pim kinases and will potentially serve as a starting point for a new class of anti-cancer therapeutics.

Acknowledgment—We thank Dr. Kunde Guo for cloning and expression testing of Pim-1 constructs.

REFERENCES

1. Cuypers, H. T., Selten, G., Quint, W., Zijlstra, M., Maandag, E. R., Boelens, W., van Wezenbeek, P., Melief, C., and Berns, A. (1984) *Cell* **37,** 141–150
2. van Lohuizen, M., Verbeek, S., Krimpenfort, P., Domen, J., Saris, C., Radaszkiewicz, T., and Berns, A. (1989) *Cell* **56,** 673–682
3. Verbeek, S., van Lohuizen, M., van der Valk, M., Domen, J., Kraal, G., and Berns, A. (1991) *Mol. Cell. Biol.* **11,** 1176–1179
4. Breuer, M. L., Cuypers, H. T., and Berns, A. (1989) *EMBO J.* **8,** 743–748
5. Mikkers, H., Allen, J., Knipscheer, P., Romeijn, L., Hart, A., Vink, E., and Berns, A. (2002) *Nat. Genet.* **32,** 153–159
6. Amson, R., Sigaux, F., Przedborski, S., Flandrin, G., Givol, D., and Telerman, A. (1989) *Proc. Natl. Acad. Sci. U. S. A.* **86,** 8857–8861
7. Cohen, A. M., Grinblat, B., Bessler, H., Kristt, D., Kremer, A., Schwartz, A., Halperin, M., Shalom, S., Merkel, D., and Don, J. (2004) *Leuk. Lymphoma* **45,** 951–955
8. Dhanasekaran, S. M., Barrette, T. R., Ghosh, D., Shah, R., Varambally, S., Kurachi, K., Pienta, K. J., Rubin, M. A., and Chinnaiyan, A. M. (2001) *Nature* **412,** 822–826
9. Ellwood-Yen, K., Graeber, T. G., Wongvipat, J., Iruela-Arispe, M. L., Zhang, J., Matusik, R., Thomas, G. V., and Sawyers, C. L. (2003) *Cancer Cell* **4,** 223–238
10. Fujii, C., Nakamoto, Y., Lu, P., Tsuneyama, K., Popivanova, B. K., Kaneko, S., and Mukaida, N. (2005) *Int. J. Cancer* **114,** 209–218
11. Pasqualucci, L., Neumeister, P., Goossens, T., Nanjangud, G., Chaganti, R. S., Kuppers, R., and Dalla-Favera, R. (2001) *Nature* **412,** 341–346
12. Akasaka, H., Akasaka, T., Kurata, M., Ueda, C., Shimizu, A., Uchiyama, T., and Ohno, H. (2000) *Cancer Res.* **60,** 2335–2341
13. Giles, F. (2005) *Blood* **105,** 4158–4159
14. Kumar, A., Mandiyan, V., Suzuki, Y., Zhang, C., Rice, J., Tsai, J., Artis, D. R., Ibrahim, P., and Bremer, R. (2005) *J. Mol. Biol.* **348,** 183–193
15. Bullock, A. N., Debreczeni, J. É., Fedorov, O. Y., Nelson, A., Marsden, B. D., and Knapp, S. (2005) *J. Med. Chem.*, in press.
16. Allen, J. D., Verhoeven, E., Domen, J., van der Valk, M., and Berns, A. (1997) *Oncogene* **15,** 1133–1141
17. Bachmann, M., and Moroy, T. (2005) *Int. J. Biochem. Cell Biol.* **37,** 726–730
18. Wang, Z., Bhattacharya, N., Weaver, M., Petersen, K., Meyer, M., Gapter, L., and Magnuson, N. S. (2001) *J. Vet. Sci.* **2,** 167–179
19. Zhu, N., Ramirez, L. M., Lee, R. L., Magnuson, N. S., Bishop, G. A., and Gold, M. R. (2002) *J. Immunol.* **168,** 744–754
20. Fox, C. J., Hammerman, P. S., Cinalli, R. M., Master, S. R., Chodosh, L. A., and Thompson, C. B. (2003) *Genes Dev.* **17,** 1841–1854
21. Mikkers, H., Nawijn, M., Allen, J., Brouwers, C., Verhoeven, E., Jonkers, J., and Berns, A. (2004) *Mol. Cell. Biol.* **24,** 6104–6115
22. Koike, N., Maita, H., Taira, T., Ariga, H., and Iguchi-Ariga, S. M. (2000) *FEBS Lett.* **467,** 17–21
23. Leverson, J. D., Koskinen, P. J., Orrico, F. C., Rainio, E. M., Jalkanen, K. J., Dash, A. B., Eisenman, R. N., and Ness, S. A. (1998) *Mol. Cell* **2,** 417–425
24. Rainio, E. M., Sandholm, J., and Koskinen, P. J. (2002) *J. Immunol.* **168,** 1524–1527
25. Winn, L. M., Lei, W., and Ness, S. A. (2003) *Cell Cycle* **2,** 258–262
26. Bachmann, M., Hennemann, H., Xing, P. X., Hoffmann, I., and Moroy, T. (2004) *J. Biol. Chem.* **279,** 48319–48328
27. Mochizuki, T., Kitanaka, C., Noguchi, K., Muramatsu, T., Asai, A., and Kuchino, Y. (1999) *J. Biol. Chem.* **274,** 18659–18666
28. Wang, Z., Bhattacharya, N., Mixter, P. F., Wei, W., Sedivy, J., and Magnuson, N. S. (2002) *Biochim. Biophys. Acta* **1593,** 45–55
29. Aho, T. L., Sandholm, J., Peltola, K. J., Mankonen, H. P., Lilly, M., and Koskinen, P. J. (2004) *FEBS Lett.* **571,** 43–49
30. Yan, B., Zemskova, M., Holder, S., Chin, V., Kraft, A., Koskinen, P. J., and Lilly, M. (2003) *J. Biol. Chem.* **278,** 45358–45367
31. Chen, X. P., Losman, J. A., Cowan, S., Donahue, E., Fay, S., Vuong, B. Q., Nawijn, M. C., Capece, D., Cohan, V. L., and Rothman, P. (2002) *Proc. Natl. Acad. Sci. U. S. A.* **99,** 2175–2180
32. Friedmann, M., Nissen, M. S., Hoover, D. S., Reeves, R., and Magnuson, N. S. (1992) *Arch. Biochem. Biophys.* **298,** 594–601
33. Palaty, C. K., Clark-Lewis, I., Leung, D., and Pelech, S. L. (1997) *Biochem. Cell Biol.* **75,** 153–162
34. Hutti, J. E., Jarrell, E. T., Chang, J. D., Abbott, D. W., Storz, P., Toker, A., Cantley, L. C., and Turk, B. E. (2004) *Nat. Methods* **1,** 27–29
35. Alessi, D. R., Caudwell, F. B., Andjelkovic, M., Hemmings, B. A., and Cohen, P. (1996) *FEBS Lett.* **399,** 333–338
36. Obata, T., Yaffe, M. B., Leparc, G. G., Piro, E. T., Maegawa, H., Kashiwagi, A., Kikkawa, R., and Cantley, L. C. (2000) *J. Biol. Chem.* **275,** 36108–36115
37. Hammerman, P. S., Fox, C. J., Birnbaum, M. J., and Thompson, C. B. (2005) *Blood* **105,** 4477–4483
38. Hammerman, P. S., Fox, C. J., Cinalli, R. M., Xu, A., Wagner, J. D., Lindsten, T., and Thompson, C. B. (2004) *Cancer Res.* **64,** 8341–8348
39. Jacobs, M. D., Black, J., Futer, O., Swenson, L., Hare, B., Fleming, M., and Saxena, K.

(2005) *J. Biol. Chem.* **280,** 13728–13734
40. Qian, K. C., Wang, L., Hickey, E. R., Studts, J., Barringer, K., Peng, C., Kronkaitis, A., Li, J., White, A., Mische, S., and Farmer, B. (2005) *J. Biol. Chem.* **280,** 6130–6137
41. Yang, J., Cron, P., Good, V. M., Thompson, V., Hemmings, B. A., and Barford, D. (2002) *Nat. Struct. Biol.* **9,** 940–944
42. Brown, N. R., Noble, M. E., Endicott, J. A., and Johnson, L. N. (1999) *Nat. Cell Biol.* **1,** 438–443
43. Lowe, E. D., Noble, M. E., Skamnaki, V. T., Oikonomakos, N. G., Owen, D. J., and Johnson, L. N. (1997) *EMBO J.* **16,** 6646–6658
44. Madhusudan, Trafny, E. A., Xuong, N. H., Adams, J. A., Ten Eyck, L. F., Taylor, S. S., and Sowadski, J. M. (1994) *Protein Sci.* **3,** 176–187
45. Leslie, A. G. W. (1992) in *Joint CCP4 and ESF-EAMCB Newsletter on Protein Crystallography*, Vol. 26, Daresbury Laboratory, Warrington, UK
46. Evans, P. R. (1993) *Proceedings of CCP4 Study Weekend on Data Collection & Processing*, pp. 114–122
47. CCP4 (1994) *Acta Crystallogr. D Biol. Crystallogr.* **50,** 760–763
48. Storoni, L. C., McCoy, A. J., and Read, R. J. (2004) *Acta Crystallogr. D Biol. Crystallogr.* **60,** 432–438
49. Murshudov, G. N., Vagin, A. A., and Dodson, E. J. (1997) *Acta Crystallogr. D Biol. Crystallogr.* **53,** 240–255
50. McRee, D. E. (1999) *J. Struct. Biol.* **125,** 156–165
51. Ross, H., Armstrong, C. G., and Cohen, P. (2002) *Biochem. J.* **366,** 977–981
52. Palaty, C. K., Kalmar, G., Tai, G., Oh, S., Amankawa, L., Affolter, M., Aebersold, R., and Pelech, S. L. (1997) *J. Biol. Chem.* **272,** 10514–10521
53. Knighton, D. R., Zheng, J. H., Ten Eyck, L. F., Xuong, N. H., Taylor, S. S., and Sowadski, J. M. (1991) *Science* **253,** 414–420
54. Fujii, K., Zhu, G., Liu, Y., Hallam, J., Chen, L., Herrero, J., and Shaw, S. (2004) *Proc. Natl. Acad. Sci. U. S. A.* **101,** 13744–13749
55. Zhu, G., Fujii, K., Belkina, N., Liu, Y., James, M., Herrero, J., and Shaw, S. (2005) *J. Biol. Chem.* **280,** 10743–10748
56. Manning, G., Whyte, D. B., Martinez, R., Hunter, T., and Sudarsanam, S. (2002) *Science* **298,** 1912–1934
57. Dale, S., Wilson, W. A., Edelman, A. M., and Hardie, D. G. (1995) *FEBS Lett.* **361,** 191–195
58. Manke, I. A., Nguyen, A., Lim, D., Stewart, M. Q., Elia, A. E., and Yaffe, M. B. (2005) *Mol. Cell* **17,** 37–48
59. Nishikawa, K., Toker, A., Johannes, F. J., Songyang, Z., and Cantley, L. C. (1997) *J. Biol. Chem.* **272,** 952–960
60. Tessmer, G. W., Skuster, J. R., Tabatabai, L. B., and Graves, D. J. (1977) *J. Biol. Chem.* **252,** 5666–5671
61. White, R. R., Kwon, Y. G., Taing, M., Lawrence, D. S., and Edelman, A. M. (1998) *J. Biol. Chem.* **273,** 3166–3172
62. Domen, J., van der Lugt, N. M., Laird, P. W., Saris, C. J., Clarke, A. R., Hooper, M. L., and Berns, A. (1993) *Blood* **82,** 1445–1452
63. Fox, C. J., Hammerman, P. S., and Thompson, C. B. (2005) *J. Exp. Med.* **201,** 259–266
64. Parang, K., and Cole, P. A. (2002) *Pharmacol. Ther.* **93,** 145–157
65. Abagyan, R., Totrov, M., and Kuznetsov, D. (1994) *J. Comput. Chem.* **15,** 488–506

Structure and Substrate Specificity of the Pim-1 Kinase

Alex N. Bullock, Judit Debreczeni, Ann L. Amos, Stefan Knapp and Benjamin E. Turk

J. Biol. Chem. 2005, 280:41675-41682.
doi: 10.1074/jbc.M510711200 originally published online October 13, 2005
